Provided for non-commercial research and education use.
Not for reproduction, distribution or commercial use.

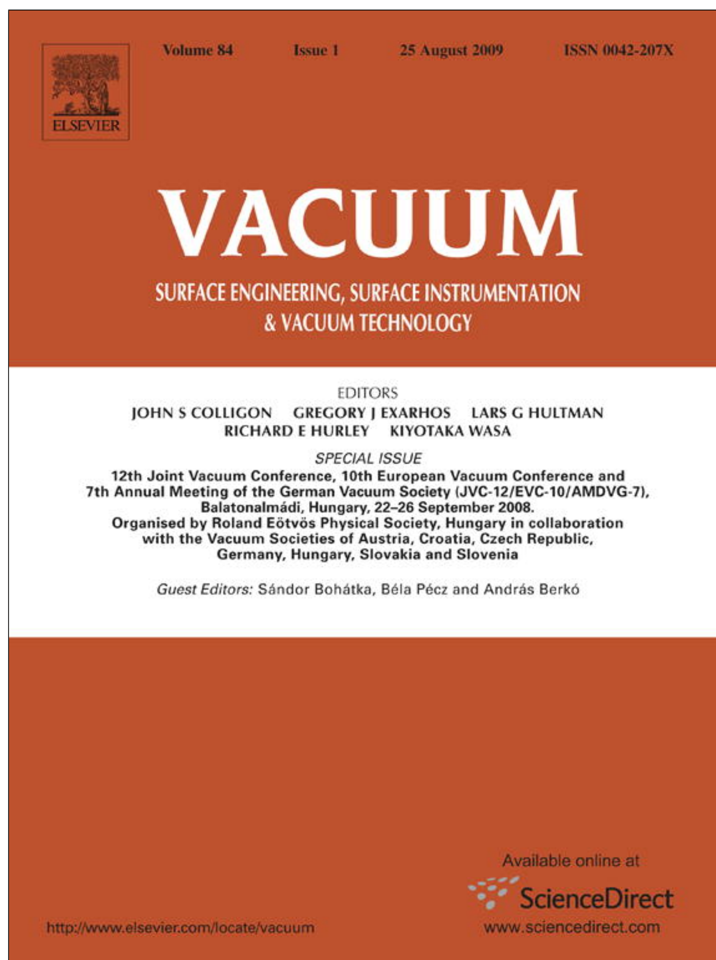

This article appeared in a journal published by Elsevier. The attached copy is furnished to the author for internal non-commercial research and education use, including for instruction at the authors institution and sharing with colleagues.

Other uses, including reproduction and distribution, or selling or licensing copies, or posting to personal, institutional or third party websites are prohibited.

In most cases authors are permitted to post their version of the article (e.g. in Word or Tex form) to their personal website or institutional repository. Authors requiring further information regarding Elsevier's archiving and manuscript policies are encouraged to visit:

http://www.elsevier.com/copyright

Author's personal copy

Vacuum 84 (2010) 243–246

Contents lists available at ScienceDirect

Vacuum

journal homepage: www.elsevier.com/locate/vacuum

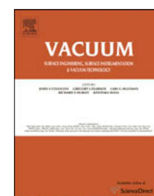

DC conductivity of amorphous–nanocrystalline silicon thin films

D. Gracin [a], B. Etlinger [a,*], K. Juraić [a], A. Gajović [a], P. Dubček [a], S. Bernstorff [b]

[a] Ruđer Bošković Institute, 10000 Zagreb, Bijenička c. 54, Croatia
[b] Sincrotrone Trieste, SS 14, km 163.5, Basovizza (TS), Italy

Keywords:
Nanocrystalline silicon
DC conductivity
Crystallinity
Raman
GISAXS

A B S T R A C T

The direct current (DC) conductivity of amorphous–nanocrystalline Si films deposited by the plasma enhanced chemical vapour deposition method was studied as a function of the structural properties obtained by Raman spectroscopy and grazing incidence small angle X-ray scattering (GISAXS).
The crystalline fraction estimated from the Raman spectra altered between 0 and 60% while the average size of the crystals varied from 2 to 7 nm, however, the size distribution was wide i.e. smaller and larger crystals were also present.
GISAXS showed a signal that corresponds to "particles" with values for the gyration radius close to the average crystal sizes, between 2 and 6 nm. Samples with higher crystalline fraction had elongated "particles" that are larger when situated closer to the sample surface, which indicates a columnar structure.
The DC conductivity had a nearly constant, low value up to some 30% of crystal fraction. A further increase of the crystal fraction resulted in an abrupt increase of the conductivity in a narrow interval of crystal fraction. Above this interval, conductivity was much higher and remained constant in that range. This result is in perfect agreement with the percolation threshold obtained by model calculation for a six-fold coordinated cubic lattice that appears at 32% of crystal fraction. A certain scattering of the experimental data around the predicted values was discussed as a possible consequence of the variation of the individual crystal size and shape by change of the crystal fraction and/or non-uniformity of depth distribution.

© 2009 Elsevier Ltd. All rights reserved.

1. Introduction

The discussion about conductivity of amorphous–nanocrystalline Si thin films deposited by PECVD (Plasma Enhanced Chemical Vapour Deposition) is accompanied by controversy since the system is not well defined. The amorphous matrix as well as the nature and shape of the nano-crystals are different from sample to sample assuming microscopic inhomogeneities. During formation, the crystalline part usually starts growing from seeds formed close to the substrate in columnar-like structure [1]. The columns are equal in thickness, or the column diameter gradually increases during formation. For the same crystal to amorphous volume fraction, the individual crystal sizes can be different, depending on the ratio between nucleation and individual crystal growth; if nucleation prevails, the structure consists of more smaller crystals and vice-versa. Furthermore, the amorphous matrix could have various degrees of structural ordering and its contribution to the transport properties could be different for the same crystal to amorphous ratio [2].

In order to test the validity of percolation theory for describing nanocrystalline samples, we deposited thin silicon films with isolated nano-crystals embedded in amorphous silicon matrix. These structures remain nearly the same up to 60% of crystal fraction, enabling a comparison with the model calculation recently done by Shimakawa [3,4].

2. Experimental

A series of multilayered silicon thin films were prepared by decomposition of silane gas, diluted with hydrogen, in a radio-frequency (RF) glow discharge, as explained in more detail previously [5–7]. Samples with different crystallinity and individual crystal sizes in the nanocrystalline silicon (*nc*-Si) layer were prepared by changing the RF plasma power density and/or the SiH/H ratio. Some of the samples were deposited by micro-wave plasma enhanced chemical vapour deposition (MWPECVD), in the way described in ref. [8]. The thickness of the deposited films was between 70 and 500 nm.

* Corresponding author. Tel.: +385 4560970.
E-mail address: etlinger@irb.hr (B. Etlinger).

0042-207X/$ – see front matter © 2009 Elsevier Ltd. All rights reserved.
doi:10.1016/j.vacuum.2009.04.008

Author's personal copy

The nanostructure of deposited films was studied using Raman spectroscopy (RS), and grazing incidence small angle X-ray spectroscopy (GISAXS), while DC conductivity was performed at room temperature by a conventional method using two metal strips on the surface of the thin films. Since the geometry in this way is not optimal, in the discussion we use the relative dependence of the resistance.

Raman spectroscopy was carried out using a computerized DILOR Z24 triple monochromator with a Coherent INNOVA 400 argon-ion laser, operating at the 514.5 nm line for excitation. In order to prevent structural changes of the samples due to heating in the laser beam during the recording of the spectra, the incident laser beam was focused with an astigmatic lens into a line shape of $50 \times 3000\ \mu m^2$, thus keeping the laser-power density below $100\ W\,cm^{-2}$.

GISAXS measurements were performed at the synchrotron ELETTRA, Trieste (Italy), at the SAXS beam-line [9] using an X-ray beam energy of 8 keV that corresponds to the wavelength $\lambda = 0.154$ nm. The grazing angle of incidence, α_i, was selected in the range $0.4° < \alpha_i < 1.4°$. X-ray scattering intensity spectra were acquired by a 2D position sensitive charge-coupled device (CCD) detector, at a detector-to-sample distance $L = 2$ m. By changing the grazing incident angle, it is possible to obtain the depth distribution of the 'particle' sizes. The GISAXS intensity is a convolution of scattering contributions from different depths attenuated according to the incoming and scattering angle. Therefore, an evaluation of the precise values would be very demanding and time consuming. However, for a rough estimation, the dominant contribution at the critical grazing incident angle comes from the near surface layer, while at the widest angles the contribution from the layer that is 300–400 nm below the surface becomes significant. The 'particle' sizes in the direction parallel to the surface and perpendicular to it were estimated by using the Guinier approximation for the analysis of the one-dimensional intensity distribution in two characteristic directions, parallel and perpendicular to the surface [10].

3. Results and discussion

3.1. Raman spectroscopy measurements

A typical Raman spectrum of a sample with 50% crystalline phase is plotted in Fig. 1 with full circles. With lines are plotted the best mathematical fit to the data that represent the amorphous phase as a sum of 4 Gauss-like peaks that correspond to the LO, LA, TO and TA vibrations, centered around 150, 310, 400 and 480 cm^{-1}, respectively. In Fig. 1 is also plotted the difference between the measured spectrum and the amorphous phase, which therefore corresponds to the nanocrystalline phase and has a peak in the range between 500 and 520 cm^{-1}. The peak position was used for the estimation of the average crystal size, D_R, by using the empirical relation [11]:

$$D_R = 2\pi\sqrt{\frac{2.2}{(522 - \omega_{TO})}} \quad (1)$$

where ω_{TO} is the frequency of the TO peak position.

The crystal fractions of the deposited samples, X_C, were estimated as the ratio between the areas of the TO phonon peak that corresponds to the crystalline fraction, $A_{TO\ cryst}$ and those that correspond to the amorphous fraction, $A_{TO\ amorphous}$, using the simple relation:

Table 1
Crystal volume fraction, X_C, Raman crystal size D_R, GISAXS gyration radius R_{GAVER}, resistivity and way of deposition of the amorphous–nanocrystalline thin films.

Crystal. fraction X_C	Raman crystal size (nm)	GISAXS radius of gyration (nm)	Resistivity (Ω cm)	Deposition technique
0.00	0.0		8.30E + 08	MW
0.00	0.0		1.00E + 09	MW
0.02	2.0		1.40E + 08	RF
0.03	2.0		3.20E + 08	RF
0.05	2.0		1.00E + 08	RF
0.07	3.2	3.6	5.00E + 07	MW
0.10	1.6		2.00E + 08	MW
0.20			2.60E + 08	RF
0.22			1.10E + 08	RF
0.26	5.7	5.5	1.30E + 08	RF
0.28	2.6	2	5.20E + 08	RF
0.31	3.5		7.00E + 06	RF
0.32	4.6	4.2	3.30E + 07	RF
0.33	3.5		4.50E + 06	RF
0.40	7.0		1.60E + 06	RF
0.46	3.2		6.00E + 05	MW
0.59	4.0	3.7	3.30E + 05	MW
0.61	3.0	3.9	2.50E + 05	MW

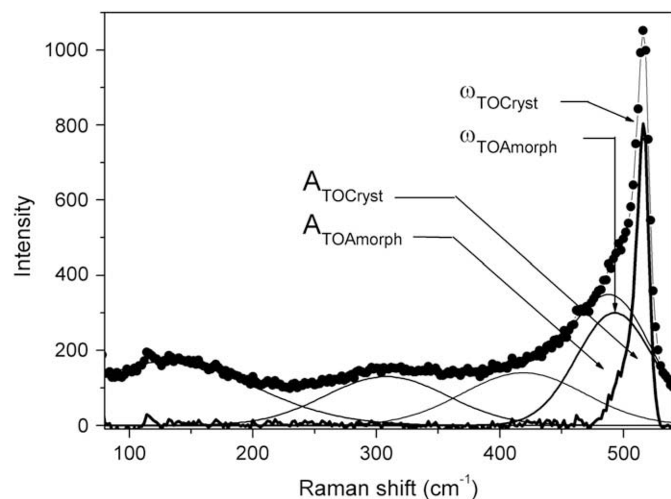

Fig. 1. Raman spectra of amorphous–nanocrystalline sample with $X_C \approx 50\%$ (full circles) and mathematical fit by 4 Gaussian curves for the amorphous phase and the difference for the nano-crystals (straight lines).

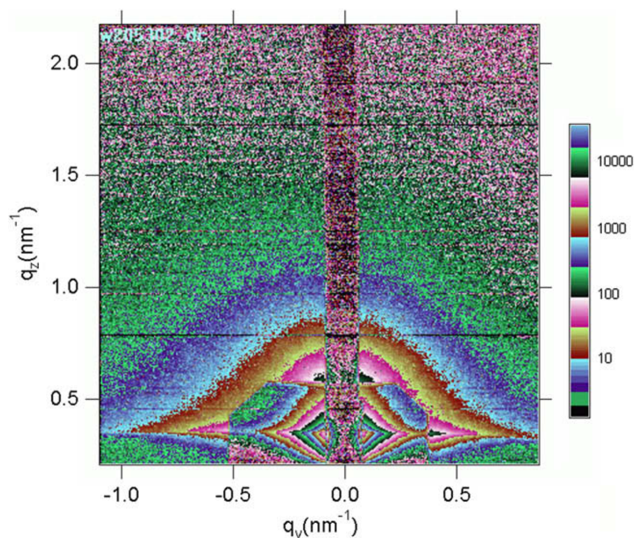

Fig. 2. 2D GISAXS pattern of a sample with $X_C \approx 26\%$.

Author's personal copy

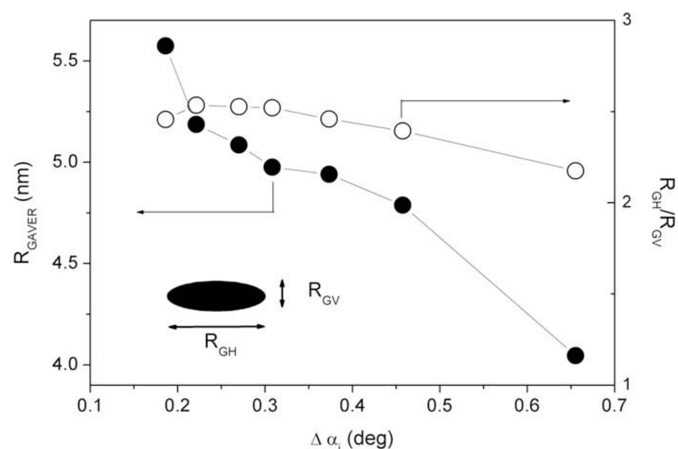

Fig. 3. Average radius of gyration, R_{GAV} (full circles) and ratio between the radius of gyration parallel to the surface, R_{GH}, and perpendicular to the surface, R_{GV} (open symbols) as a function of the difference between the applied and the critical GISAXS angle.

$$X_C = \frac{A_{TO\ cryst}}{\left(A_{TO\ cryst} + \beta A_{TO\ amorphous}\right)} \quad (2)$$

β stands for the balance between the cross-section of the amorphous and crystalline phase. We took as first approximation the value $\beta = 1$, since this approach resulted in reasonable agreement with values estimated from optical measurements [12]. The results obtained from Raman measurements are summarized in the first and second column of Table 1 showing that the average crystal size gradually increases with the crystalline fraction.

3.2. GISAXS measurements

A typical GISAXS pattern for a sample with a high crystalline fraction is shown in Fig. 2. It was taken at a grazing incidence angle 0.5° above the critical angle. Here $q = 4\pi \sin \theta/\lambda$ is the modulus of the scattering vector, 2θ is scattering angle and λ is X-ray wavelength. With q_z and q_x are denoted the components perpendicular and parallel to the sample surface, respectively. The colours represent the intensity according to the given scale,

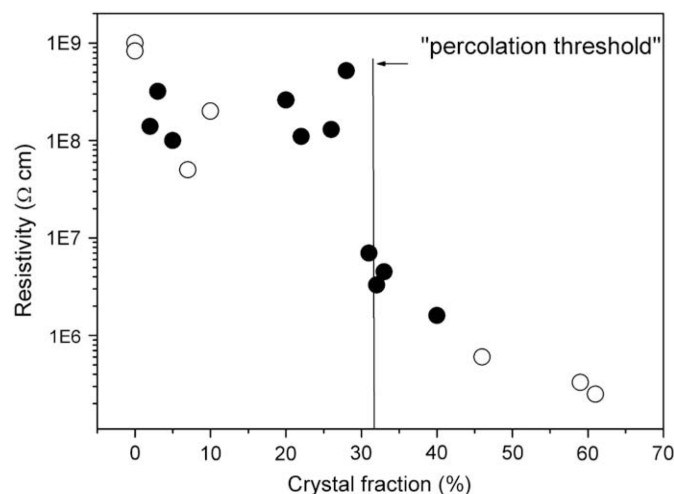

Fig. 4. Resistivity versus crystal volume fraction; full symbols are for RF PECVD while open symbols are for MW PECVD samples.

enabling a 3D representation. By analyzing the one-dimensional intensity distribution in q_z and q_x directions using the Guinier approximation [10] the particles size and shape were estimated. The particle size is represented by the radius of gyration R_G, which is proportional to the actual size through a relation which depends on the exact shape of the particle. The average R_G values are plotted in Fig. 3 for a sample with 46% of crystal fraction as a function of the grazing incidence angle. The angles close to zero correspond to the sample surface while the highest angle in the plot corresponds to the part of the sample that is several hundreds of nanometers below the surface. From Fig. 3 it can be seen that the average particle sizes (full circles) are larger for lower angles, e.g. closer to surface. The shape of the particles is ellipsoidal, as can be seen from the ratio between the size of horizontal (RH) and vertical direction (RV) plotted as open circles. This anisotropy is larger for lower angles. GISAXS was performed on a representative set of samples, and the average R_G values are given in Table 1. The size values obtained by Raman, D_R, and the average GISAXS radii, R_{GAVER}, are very similar as can be seen comparing the values in second and third columns of Table 1. This fact suggests that the "particles" seen by GISAXS are single nano-crystals embedded in amorphous matrix.

3.3. Conductivity measurements

The measured resistivity of the samples is given in Table 1 and plotted in Fig. 4 as a function of the crystal fraction X_C. For low X_C, the resistivity is high and almost constant up to 30%. At this value, the resistivity drops by several orders of magnitude in a narrow interval of crystal fraction and decreases gradually further for larger X_C. This behaviour can be explained by the percolation theory [13]. The model assumes high conductive particles placed in a low-conductive matrix. For a low concentration of the conductive particles, there is practically no influence of the highly conductive particles on the conductivity. When the number of conductive particles increase up to certain level, the probability for mutual connection increases and thus the conductivity of the complete layer abruptly increases. This event is called "percolation threshold" and appears in 2D models between 40 and 45% volume contribution of conductive particles [13]. Recent calculations for 3D silicon [3,4,14,15] give a threshold value between 32 and 33%, which is in perfect agreement with our results.

This agreement confirms our way for the estimation of the crystal fraction by Raman where the key assumption was a similarity in the cross-sections for nano-crystals of 2–7 nm (actual size) and amorphous matrix. Also the possibility to explain our conductivity measurements with a percolation model supports our assumption that the particles seen by GISAXS are actually nano-crystals.

4. Conclusion

The structural properties and DC conductivity of thin amorphous–nanocrystalline Si films deposited by the PECVD method were measured. The crystal fraction estimated by Raman spectroscopy was from 0 to 60% while the Raman crystal size varied from 2 to 7 nm. GISAXS patterns corresponded to "particles" with a similar size as the nano-crystals, which suggest that the "particles" and crystals are the same objects. The dependence of the DC conductivity on the crystal fraction agreed perfectly with the 3D percolation theory, and the percolation threshold is close to 30% of volume crystal fraction.

Author's personal copy

Acknowledgments

This work was supported by the Croatian Ministry of Science Education and Sport, grants "The thin film silicon on the amorphous to crystalline transition" (098-0982886-2894) and "Physics and applications of nanostructures and bulk matter" (098-0982904-2898).

References

[1] Fejfar A, Mates T, Čertik O, Rezek B, Stuchlik J, Pelant I, et al. J Non-Cryst Solids 2004;338–340:303.
[2] Gracin D, Etlinger B, Juraic K, Gajovic A, Dubcek P, Bernstorff S. Vacuum 2008;82:205.
[3]. Shimakawa K. J Non-Cryst Solids 2000;266–269:223.
[4] Shimakawa K. In: IEEE, Canadian conference on electrical and computer engineering, Saskaton; 1–4 May 2005. p. 348.
[5] Gracin D, Bernstorff S, Dubcek P, Gajovic A, Juraic K. J Appl Cryst 2007;40:373.
[6] Gracin D, Bernstorff S, Dubcek P, Gajovic A, Juraic K. Thin Solid Films 2007;515:5615.
[7] Gracin D, Juraic K, Dubcek P, Gajovic A, Bernstorff S. Appl Surf Sci 2006;252:5598.
[8] Soppe WJ, Biebericher ACW, Devilee C, Donker H, Schlemm H. In: Proc. of third world conf. on photovoltaic energy conversion (IEEE cat. no 03CH37497), vol. 2. Arisumi Printing Inc.; 2003. p. 1655–8.
[9] Amenitsch H, Bernstorff S, Laggner P. Rev Sci Instrum 1995;66:1624.
[10] Guinier A, Fournet SG. Small-angle scattering of X-rays. New York: Wiley; 1955.
[11] Tsu R, Gonzalez-Hernandez J, Chao SS, Lee SC, Tanaka K. Appl Phys Lett 1982;40:534.
[12] Gracin D, Gajovic A, Juraic K, Ceh M, Remes Z, Poruba A, et al. J Non-Cryst Solids 2008;19–25:2286.
[13] Essam JW. Rep Prog Phys 1980;43:833.
[14] Overhof H, Otte M, Schmidtke M, Backhausen U, Carius. J Non-Cryst Solids 1998;227–230:992.
[15] Sahini M. Application of percolation theory. Washington, DC: Taylor and Francis; 1994.